Research Square

Preprints are preliminary reports that have not undergone peer review.
They should not be considered conclusive, used to inform clinical practice,
or referenced by the media as validated information.

Role of Arterial Spin Labelling (ASL) Magnetic Resonance Imaging and Magnetic Resonance Spectroscopy (MRS) in Alzheimer's disease and frontotemporal dementia

Jaya Logre
Govind Ballabh Pant Hospital
Anju Ranga
dranjuranga@gmail.com

Govind Ballabh Pant Hospital
Pranav Gupta
Govind Ballabh Pant Hospital
Poonam Narang
Govind Ballabh Pant Hospital
Kalpana Bansal
Govind Ballabh Pant Hospital
Debashish Chowdhury
Govind Ballabh Pant Hospital
Agrima Bansal
Govind Ballabh Pant Hospital

Research Article

Keywords:

Posted Date: July 27th, 2026

DOI: https://doi.org/10.21203/rs.3.rs-10416884/v1

License: This work is licensed under a Creative Commons Attribution 4.0 International License.
Read Full License

Additional Declarations: No competing interests reported.

Abstract

BACKGROUND:

Early differentiation between Alzheimer's disease (AD) and fronto-temporal dementia (FTD) remains challenging due to overlapping clinical features and structural MRI findings. Functional MRI techniques such as arterial spin labelling (ASL) and proton magnetic resonance spectroscopy (^{1}H-MRS) offer non-invasive assessment of cerebral perfusion and metabolism that may precede overt structural changes.

OBJECTIVE:

To evaluate the role of ASL and ^{1}H-MRS in early detection and differentiation of AD and FTD, and distinguishing these entities from age-related changes.

METHODS:

Fifteen patients each with AD, FTD and healthy controls underwent 3D-Pseudocontinous ASL-MRI and MRS in addition to routine imaging on 3T MRI system. Visual rating scales were used for assessment of regional atrophy. Regional cerebral blood flow (CBF) was quantified using ASL, and metabolite ratios (NAA/Cr, mI/Cr, NAA/mI) were assessed in the anterior and posterior cingulate gyri using MRS. Diagnostic performance was evaluated using receiver operating characteristic (ROC) analysis.

RESULTS:

FTD demonstrated predominant frontal and anterior temporal atrophy with corresponding hypoperfusion, while AD showed parietotemporal and posterior cingulate involvement. Mean CBF in the anterior cingulate gyrus differentiated FTD from controls with a sensitivity of 86.6% and specificity of 80% at cut-off of 31.91 ml/100 g/min. Posterior cingulate hypoperfusion differentiated AD from controls with a sensitivity of 86.6% and specificity of 73.3% at cut-off of 38.29 ml/100 g/min. On MRS, NAA/mI ratio was significantly decreased in anterior cingulate gyrus in FTD compared to both AD and controls at cut-off value of 8.56 in controls with a specificity and sensitivity of 86.6 % and 83.3% respectively, whereas in AD patients, cutoff value was 14.75 with sensitivity and specificity of 86.6% each.

CONCLUSION:

The use of functional neuroimaging techniques as an adjunct to conventional MRI can provide unique insights into the changes seen in neurodegenerative diseases in the form of disease-specific patterns of differences in perfusion and metabolism.

INTRODUCTION

Dementia is a neurodegenerative disorder characterized by progressive deterioration of cognitive functions, memory, language, praxis, and most notably the executive functions, with resultant

impairment to perform activities of daily living. There is growing interest in understanding the pathophysiology and characterizing the type of dementia so as to provide the correct disease modifying treatments, improve the clinical outcomes and patient care.

Alzheimer's disease (AD) is commonly seen in elderly, usually after 60 years of age, with increasing incidence with age. [1] Frontotemporal dementia (FTD) is the second or third most prevalent dementia subtype amongst early-onset dementias (patient age < 65 years), with up to 40% of cases having a positive family history. The diagnosis is challenging because of close similarities of behavioural changes in patients with FTD and those with psychiatric disorders.[2]

Structural MRI plays an essential role in excluding secondary causes of cognitive impairment and in identifying characteristic patterns of cerebral atrophy. However, structural changes may be subtle or absent in early disease, limiting sensitivity. Functional imaging techniques such as Flouro-deoxy Glucose Positron Emission Tomography (FDG-PET) and Single Photon Emission Computed Tomography (SPECT) can detect hypometabolism or hypoperfusion but are limited by their high cost, less availability and radiation exposure. Arterial spin labelling (ASL) MRI is a non-invasive perfusion technique that uses magnetically labelled arterial blood water as an endogenous tracer to quantify cerebral blood flow (CBF), providing information comparable to FDG-PET-based perfusion without ionising radiation. Arterial spin labelling (ASL) MRI has emerged as a non-invasive alternative capable of measuring cerebral blood flow (CBF), with growing evidence showing strong spatial concordance between ASL hypoperfusion and FDG-PET hypometabolism patterns in both AD and FTD.[4]

ASL has also been employed in large-scale studies, including Alzheimer's Disease Neuroimaging Initiative(ADNI), to examine brain function by quantifying regional CBF, complementing structural MRI and molecular imaging, thus providing information on perfusion alterations related to key AD biomarkers.[27] While the performance of ASL was worse than FDG-PET in clinching a final diagnosis, it still exhibited a decent diagnostic performance to justify its usage as a further investigation being quicker and a more convenient alternative.[5]

Proton magnetic resonance spectroscopy (^{1}H-MRS) enables in vivo assessment of brain metabolites, including N-acetyl aspartate (NAA) as a marker of neuronal integrity and myo-inositol (mI) as a marker of gliosis. Metabolic alterations detected by MRS may precede atrophy and therefore offer potential biomarkers for early disease detection.

Proton magnetic resonance spectroscopy (^{1}H-MRS) provides complementary metabolic information by quantifying neuronal integrity by concentration of N-acetyl aspartate (NAA), gliosis by Myo-inositol levels (mI) and energy metabolism by creatine (Cr), which also acts as a reference value. Prior studies have demonstrated reduced NAA and increased mI in AD and FTD; however, most investigations have focused on single modalities or limited regional assessments, and the combined diagnostic utility of ASL-MRI and MRS remains insufficiently explored.[4]

METHODOLOGY

This cross-sectional observational study was conducted between April 2023 and November 2024 at the Neurology OPD of Govind Ballabh Pant Hospital and the associated Lok Nayak Hospital, New Delhi. A total of 50 participants aged ≥ 40 years with cognitive complaints, along with age- and sex-matched healthy controls, were screened for inclusion. Participants aged **≥ 40 years** were recruited to allow inclusion of early-onset dementia cases, particularly FTD, which frequently presents before 65 years of age. Although the lower age threshold may appear low for AD, this criterion ensured coverage of atypical and early-onset presentations encountered in clinical practice. Dementia severity was assessed using the Mini Mental State Examination (MMSE) and Montreal Cognitive Assessment (MoCA). Participants with MMSE scores < 24 or MoCA scores < 26 were considered potential cases, whereas those with MMSE > 24 and MoCA > 26 were included as healthy controls. To confirm clinical diagnoses, AD patients were evaluated according to the NINCDS-ADRDA criteria (2011), and FTD patients were diagnosed using the International Consensus Criteria for Behavioural Variant FTD (2011), verified by experienced neurologists.

Exclusion criteria included:

- Acute cerebrovascular events or recent stroke
- Brain tumours or head trauma
- Contraindications to MRI
- Excessive head motion during imaging
- Dementia secondary to strategic infarcts or vascular pathology

After screening, 15 AD patients, 15 FTD patients, and 15 healthy controls were included; five participants were excluded based on the criteria above.

The study was approved by the local medical ethics committee (Institutional Ethics Committee, Maulana Azad Medical College-F.1/IEC/,MAMC/MD/MS(96/02/2023)/No.327). All the participants or primary adult caregivers in case of cognitively impaired participants were explained the procedure in their vernacular language and gave their written informed consent.

IMAGE ACQUISITION:

All the participants were examined on Philips Ingenia 3 Tesla MRI system. Image acquisition was done in the following sequences:

- 3D T1 weighted (Axial, Sagittal, Coronal)– FOV of 240 x 240 x240 mm, matrix size of 240 x 240 x170 slices, voxel size of 1 x 1 x 1 mm with TR/TE- 6.7/3 ms.
- T2 weighted (Axial) -FOV of 230 x 180 x 144 mm, matrix size of 420x317x 144 mm, voxel size of 0.55 x 0.55 x 4 mm with TR/TE-2800 /100ms, Flip angle of 90 degrees.

- 3D FLAIR (Axial, Sagittal, Coronal)- FOV of 230 x 180 x 144 mm, matrix size of 208 x 208x 304 mm, voxel size of 1.2 x 1.2 x 1.2 mm with TR/TE-4800 /340ms, Flip angle of 90 degrees.
- 3D Pseudo-continuous ASL (pCASL) (Axial, Sagittal, Coronal)- FOV – 240 X 240 mm^2, voxel size of 3.75 x 3.75 x 6 mm, matrix size of 64 x 60, TR/TE- 4252/12 ms, flip angle of 90 degrees, with a label distance of 90 mm, post-labeling delay of 2000 ms.
- Multi-voxel spectroscopy was performed at an intermediate echo time (TE = 144 ms) focusing on the cingulate gyrus, chosen due to its established involvement in both AD and FTD. Voxel placement was optimized to avoid partial volume effects and CSF contamination. Metabolites analysed included N-acetyl aspartate (NAA), myo-inositol (mI), and creatine (Cr), with calculation of ratios (NAA/Cr, mI/Cr, NAA/mI) to assess neuronal integrity and gliosis.

IMAGE ANALYSIS:

Morphological analysis of patterns of regional atrophy of the brain was done using 3DT1/T2-FLAIR sequences. Atrophy scores were given according to global cortical atrophy-frontal (GCA-F), medial temporal atrophy (MTA) score and Koedam's posterior parietal atrophy score.[7,25] Measurement of Mean (uncorrected) CBF was done from the post-processing of the obtained ASL images by generation of coloured maps and drawing Region of Interest (ROI) of size ~ 20 mm^2 in the following areas of the brain: Bilateral frontal lobes, bilateral temporal lobes, bilateral parietal lobes, bilateral occipital lobes, anterior cingulate gyrus, posterior cingulate gyrus and bilateral hippocampi.

Analysis of multivoxel MR spectroscopy was done after voxel placement in the Anterior and posterior cingulate gyrus. Assessment of concentration of metabolites (NAA, Cr, mI) was done by referring the metabolite peak area to the unsuppressed water peak area acquired under the same conditions and calculation of the mI/Cr, NAA/Cr and NAA/mI ratios was done in both anterior and posterior cingulate gyrus.

DATA ANALYSIS:

Statistical analysis was performed using SPSS version 25. Normality of continuous variables was assessed using the **Shapiro–Wilk test**, given the relatively small sample size. Normally distributed variables were analysed using parametric tests, while non-parametric alternatives were applied where appropriate. Categorical variables were compared using the Chi-square test.

Group differences in regional cerebral blood flow and MR spectroscopy metabolites were analysed using **analysis of covariance (ANCOVA)** with diagnostic group as the fixed factor and age as a covariate, given the known influence of age on cerebral perfusion and brain metabolism. **Bonferroni correction** was applied for post-hoc pairwise comparisons.

Correlation analysis between imaging parameters and clinical scores (MMSE, MoCA) was performed using Pearson or Spearman correlation coefficients as appropriate.

Receiver operating characteristic (ROC) analysis was used to evaluate diagnostic performance. Area under the curve (AUC) values with 95% confidence intervals were calculated, and optimal cut-off values were determined using the Youden index. A p-value < 0.05 was considered statistically significant.

RESULTS

Participant characteristics:

Fifty participants were included in our study: 35 dementia patients, 15 healthy participants. Post hoc, 5 of the included patients were excluded due to diagnoses other than AD/ FTD or because of incomplete imaging data.

In our study of the forty-five participants included during final analysis (15 AD, 15 FTD, and 15 healthy controls).Age range was 40–86 years and the mean age differed significantly across groups, with FTD patients being younger than AD patients and controls. A male predominance was observed across all groups. Detailed demographic and clinical characteristics, including age, sex distribution, education level, MMSE, and MoCA scores, are summarised in **(**Table 1**).**

Structural MRI Findings

On comparison of atrophy on the three visual rating scales namely GCA-F, MTA and Koedam posterior parietal atrophy scale, there was significant differences in dementia patients when compared to healthy controls (p = 0.01).[7] Atrophy of frontal lobe was seen as a key imaging feature in FTD and can therefore help to differentiate AD from controls **[**Fig. 1**(a)]**. Temporal atrophy can be associated with both FTD, AD and to a lesser extent with normal aging. **[**Fig. 1**(c),2(c)]**. Parietal atrophy was seen as a key indicator of AD and can help in differentiation from FTD and healthy controls **[**Fig. 2**(a)]**. Significant parietal atrophy can be seen in the absence of visible atrophy in the medial temporal lobe (MTL), especially in younger individuals and since MTA is considered a diagnostic sign of AD, this may imply that some patients may not be diagnosed if only MTA was evaluated. Hence, addition of assessment of parietal atrophy can aid in making the diagnosis of AD. [8] Significant hippocampal atrophy was also observed in both AD as well as FTD.[28] Correlation analysis revealed a moderate negative correlation between frontal lobe CBF and GCA-F scores (‘r’ = − 0.43, ‘p’ < 0.01) and between temporal lobe CBF and MTA scores (‘r’= − 0.52, ‘p’ < 0.01), indicating reduced perfusion with increasing atrophy severity.

ASL Perfusion Findings

ASL-MRI demonstrated significant regional hypoperfusion corresponding to areas of structural atrophy. Frontal lobe CBF was significantly reduced in both FTD and AD compared with controls (‘p’ < 0.001). **[**Fig. 1**(b)].** Similarly, hypoperfusion was seen in the temporal lobes which FTD and AD which was reduced as compared to control group (‘p’ <0.001) suggesting that temporal hypoperfusion can be seen in both FTD and AD**[**Fig. 1**(d),2(d)].** Anterior cingulate gyrus hypoperfusion was more pronounced in FTD,

whereas posterior cingulate and parietal hypoperfusion predominated in AD. [Fig. 3]. In our study, corresponding hypoperfusion was also seen in bilateral hippocampi in FTD and AD as compared to controls. (Table 2) (Fig. 5e).

After adjusting for age using ANCOVA, significant group differences in cerebral blood flow persisted across frontal, temporal, parietal, occipital, hippocampal, and cingulate regions ($p < 0.01$). Age did not significantly influence CBF in most regions, indicating that the observed hypoperfusion patterns were predominantly disease-related rather than age-driven.

Region-specific perfusion patterns were observed: anterior cingulate hypoperfusion was more pronounced in FTD, whereas posterior cingulate and parietal hypoperfusion predominated in AD. However, direct age-adjusted pairwise comparisons between AD and FTD were not consistently significant, reflecting substantial overlap in perfusion patterns between the two dementia subtypes.

Mean CBF in the anterior cingulate gyrus differentiated FTD from controls with an AUC of 0.85, sensitivity of 86.6%, and specificity of 80% at a cut-off value of 31.91 ml/100 g/min(Fig. 5a). Mean CBF in the posterior cingulate gyrus differentiated AD from controls with an AUC of 0.81, sensitivity of 86.6%, and specificity of 73.3% at a cut-off value of 38.29 ml/100 g/min. (Fig. 5b).

MRS Findings

On MR spectroscopy, significant metabolic alterations were observed in both dementia groups compared to controls. (Table 3) In the anterior cingulate gyrus, FTD patients demonstrated significantly increased myo-inositol and reduced NAA concentrations, resulting in a significantly lower NAA/mI ratio compared with both AD patients and controls ($p < 0.01$). [Fig. 4**(a,b)**].

In the posterior cingulate gyrus, both AD and FTD groups showed reduced NAA/mI ratios compared to controls, consistent with neuronal dysfunction. However, no statistically significant difference in posterior cingulate NAA/mI was observed between AD and FTD after age adjustment. [Fig. 4**(c,d)**].

These findings indicate region-specific metabolic vulnerability, with predominant anterior cingulate involvement in FTD and posterior cingulate involvement in AD, though direct differentiation between AD and FTD based on single-region spectroscopy metrics remains limited.

ROC analysis showed that NAA/mI ratio in the anterior cingulate gyrus differentiated FTD from controls with an AUC of 0.88, sensitivity of 73.3%, and specificity of 93.3% at a cut-off value of 8.56 (Fig. 5c).. Differentiation between FTD and AD using the same parameter yielded an AUC of 0.94, with sensitivity and specificity of 86.6%(Fig. 5d).

DISCUSSION

Dementia is a neurodegenerative disease which manifests as cognitive decline and impairment in activities of daily living. AD and FTD are amongst the major causes of dementia and thus, distinction between the pathologies is of utmost importance for better clinical outcomes.

This study demonstrates that ASL-MRI and ^{1}H-MRS provide complementary functional information that enhances differentiation between AD and FTD beyond conventional structural MRI. Distinct perfusion and metabolic patterns were observed in disease-specific regions of vulnerability, particularly within the cingulate cortex.

In AD, there is pathological buildup of β-amyloid protein in form of plaques and tau deposition in the form of neurofibrillary tangles, which are associated with neuronal injury. The severity of biomarkers indicates neuronal injury and the likelihood of progression to AD dementia. The two major categories of Biomarkers are: (1) The biomarkers of A-β accumulation are abnormal tracer retention on amyloid PET imaging and low CSF Aβ42. (2) The biomarkers of neuronal degeneration or injury are elevated CSF tau (both total and phosphorylated tau) and decreased FDG uptake on PET, specifically involving temporo-parietal cortex; and atrophy on structural MR in a specific topographic pattern involving medial, basal and lateral temporal lobe, and medial and lateral parietal cortices.[26]

In FTD, there is frontotemporal lobar degeneration, characterized by neuronal loss, gliosis, and microvacuolar changes of frontal lobes, anterior temporal lobes, anterior cingulate cortex, and insular cortex, with various subtypes (frontotemporal lobar degeneration tau, frontotemporal lobar degeneration-TDP, and frontotemporal lobar degeneration-FUS). The most common subtype of frontotemporal lobar degeneration tau is Pick's disease- which is characterized by Pick bodies as pathological hallmark and striking knife-edge atrophy of frontal, temporal, and cingulate gyri with relative preservation of the parietal lobe. [2] These changes were also evident in our study as patterns of regional atrophy on structural imaging using three visual rating scales namely GCA-F, MTA and Koedam scale. [8]

On ASL,FTD patients showed regional atrophy and hypoperfusion in frontal and temporal lobes along with the anterior cingulate gyrus when compared to AD. On the other hand, AD patients showed atrophy in parieto-temporal predominance, involving the posterior cingulate gyrus with corresponding hypoperfusion [17]. Observed correlations between atrophy scores and regional CBF thus reinforce the close relationship between structural degeneration and functional impairment, while also highlighting the potential of ASL to detect functional changes that may precede overt atrophy. [25]

On MRS, NAA/mI ratio was significantly decreased in anterior cingulate gyrus in FTD when compared to both AD and controls. Thus, reduction of NAA/mI in the anterior cingulate gyrus can emerge as a biomarker for differentiation between FTD and AD and can further aid in the diagnosis and improving the role of imaging in dementias. NAA/mI ratio increases the usefulness of MRS for diagnosis in AD as it is independent of Cr values, which decreases the variability resulting from age and other factors without having to calculate absolute concentrations. [10] The NAA/mI ratio is shown to be a dependable diagnostic measure for AD versus controls.[20] Alterations in the metabolic markers have been identified

in all common dementias, which are detectable in preclinical and early stages of the disease and thus act as a potential biomarker for early detection and successful subsequent management. [21]

There was reduction of NAA/mI ratio in the posterior cingulate gyrus in both AD and FTD in our study. between AD and control group and between FTD and control group which suggested reduced NAA/mI in the posterior cingulate gyrus in both AD and FTD groups when compared to healthy controls. However, results were not statistically significant between the AD and FTD groups, which showed dissonance from previous studies in the literature.[12]

Although ASL-MRI and MR spectroscopy did not consistently differentiate AD from FTD on a global basis, **region-specific perfusion and metabolic patterns were observed**, particularly within the cingulate cortex. Reduced anterior cingulate perfusion and metabolism were more prominent in FTD, consistent with preferential involvement of frontal–salience networks, whereas posterior cingulate and parietal involvement predominated in AD, reflecting degeneration of the default mode network. These findings suggest that **ASL and MRS are sensitive markers of neurodegeneration but have limited specificity when used in isolation**. Their greatest clinical value lies in **supporting network-based interpretation when combined with clinical phenotype, neuropsychological testing, and structural imaging.**

Overall, our findings were consistent with prior ASL and MRS studies reporting disease-specific perfusion and metabolic patterns, though direct comparison is limited by methodological differences and sample size. Importantly, ASL and MRS offer these insights without radiation exposure, making them suitable for repeated assessments and potential use in younger or early-onset dementia populations.

Limitations

This study has several limitations, including a relatively small sample size, cross-sectional design, age differences between groups, and lack of formal dementia severity staging such as the Clinical Dementia Rating scale. The heterogeneity of our sample on the other hand indicates the complexity of this patient population and the difficulty inherent to nosological diagnosis as a reference standard and definitive histopathological diagnosis could not be done due to humanitarian reasons. MRS analysis was limited to the cingulate gyrus, and inclusion of additional regions may provide a more comprehensive metabolic profile. These factors should be addressed in future longitudinal studies.

Conclusion

ASL-MRI and ^{1}H-MR spectroscopy serve as valuable adjuncts to conventional MRI by providing non-invasive assessment of cerebral perfusion and metabolism. While both techniques effectively differentiate dementia patients from healthy controls, their ability to distinguish Alzheimer's disease from frontotemporal dementia is limited when used in isolation. Region-specific perfusion and metabolic patterns, particularly within the cingulate cortex, may provide supportive diagnostic information within a

multimodal imaging framework, enhancing understanding of network-level neurodegeneration in dementia. Their combined application improves functional differentiation between AD and FTD and holds promise as an imaging-based biomarker approach for characterising neurodegenerative dementias in clinical practice.

Declarations

Author Contribution

J.L, P.N., K.B. and D.C. made substantial contributions to the conception or design of the work, and wrote the main manuscript text.J.L., A.R., PG. contributed towards the acquisition, analysis, or interpretation of data.J.L., P.N., K.B. and A.R. wrote the manucript text.All authors reviewed the manuscript and revised it critically for important intellectual content, approved the version to be published; and agree to be accountable for all aspects of the work.

References

1. Li X, Feng X, Sun X, Hou N, Han F, Liu Y. Global, regional, and national burden of Alzheimer's disease and other dementias, 1990–2019. Front Aging Neurosci. 2022; 14:937486.
2. Bang J, Spina S, Miller BL. Frontotemporal dementia. Lancet. 2015;386(10004):1672–82.
3. Roquet D, Sourty M, Botzung A, Armspach JP, Blanc F. Brain perfusion in dementia with Lewy bodies and Alzheimer's disease: an arterial spin labeling MRI study on prodromal and mild dementia stages. Alzheimers Res Ther. 2016; 8:29.
4. Zeng HM, Han HB, Zhang QF, Bai H. Application of modern neuroimaging technology in the diagnosis and study of Alzheimer's disease. Neural Regen Res. 2021;16(1):73–9.
5. Ssali T, Anazodo UC, Narciso L, Liu L, Jesso S, Richardson L, Günther M, Konstandin S, Eickel K, Prato F, Finger E. Sensitivity of arterial spin labeling for characterization of longitudinal perfusion changes in frontotemporal dementia and related disorders. NeuroImage: Clinical. 2022;35:102853.
6. Rascovsky K, Hodges JR, Knopman D, Mendez MF, Kramer JH, Neuhaus J, et al. Sensitivity of revised diagnostic criteria for the behavioural variant of frontotemporal dementia. Brain. 2011;134(Pt 9):2456–77.
7. Živanović M, Aracki Trenkić A, Milošević V, Stojanov D, Mišić M, Radovanović M, et al. The role of magnetic resonance imaging in the diagnosis and prognosis of dementia. Biomol Biomed. 2023;23(2):209–24.
8. Yuan Z, Pan C, Xiao T, Liu M, Zhang W, Jiao B, et al. Multiple Visual Rating Scales Based on Structural MRI and a Novel Prediction Model Combining Visual Rating Scales and Age Stratification in the Diagnosis of Alzheimer's Disease in the Chinese Population. Front Neurol. 2019; 10:93.
9. Huang W, Alexander GE, Chang L, Shetty HU, Krasuski JS, Rapoport SI, et al. Brain metabolite concentration and dementia severity in Alzheimer's disease: a (1)H MRS study. Neurology.

2001;57(4):626–32.

10. Coulthard E, Firbank M, English P, Welch J, Birchall D, O'Brien J, et al. Proton magnetic resonance spectroscopy in frontotemporal dementia. J Neurol. 2006 ;253(7):861–8.
11. Kantarci K, Petersen RC, Boeve BF, Knopman DS, Tang-Wai DF, et al. 1H MR spectroscopy in common dementias. Neurology. 2004;63(8):1393–8.
12. Waragai M, Moriya M, Nojo T. Decreased N-Acetyl Aspartate/Myo-Inositol Ratio in the Posterior Cingulate Cortex Shown by Magnetic Resonance Spectroscopy May Be One of the Risk Markers of Preclinical Alzheimer's Disease: A 7-Year Follow-Up Study. J Alzheimers Dis. 2017;60(4):1411–27.
13. Haller S, Zaharchuk G, Thomas DL, Lovblad KO, Barkhof F, Golay X. Arterial Spin Labeling Perfusion of the Brain: Emerging Clinical Applications. Radiology. 2016;281(2):337–56.
14. Petcharunpaisan S, Ramalho J, Castillo M. Arterial spin labeling in neuroimaging. World J Radiol. 2010;2(10):384–98.
15. Du AT, Jahng GH, Hayasaka S, Kramer JH, Rosen HJ, Gorno-Tempini ML, et al. Hypoperfusion in frontotemporal dementia and Alzheimer disease by arterial spin labeling MRI. Neurology. 2006 ;67(7):1215–20.
16. Binnewijzend MA, Kuijer JP, Benedictus MR, van der Flier WM, Wink AM, Wattjes MP et al. Cerebral blood flow measured with 3D pseudocontinuous arterial spin-labeling MR imaging in Alzheimer disease and mild cognitive impairment: a marker for disease severity. Radiology. 2013;267(1):221–30.
17. Steketee RM, Bron EE, Meijboom R, Houston GC, Klein S, Mutsaerts HJ, et al. Early-stage differentiation between presenile Alzheimer's disease and frontotemporal dementia using arterial spin labeling MRI. Eur Radiol. 2016;26(1):244–53.
18. Burtscher IM, Holtås S. Proton MR spectroscopy in clinical routine. J Magn Reson Imaging. 2001;13(4):560–7
19. McKiernan E, Su L, O'Brien J. MRS in neurodegenerative dementias, prodromal syndromes and at-risk states: A systematic review of the literature. NMR Biomed. 2023;36(7): e4896.
20. Soher BJ, Doraiswamy PM, Charles HC. A review of 1H MR spectroscopy findings in Alzheimer's disease. Neuroimaging Clin N Am. 2005;15(4):847–52.
21. Maul S, Giegling I, Rujescu D. Proton Magnetic Resonance Spectroscopy in Common Dementias-Current Status and Perspectives. Front Psychiatry. 2020;11:769
22. Jia X, Wang Z, Huang F, Su C, Du W, Jiang H, et al. A comparison of the Mini-Mental State Examination (MMSE) with the Montreal Cognitive Assessment (MoCA) for mild cognitive impairment screening in Chinese middle-aged and older population: a cross-sectional study. BMC psychiatry. 2021;21:1–3
23. Mihara M, Hattori N, Abe K, Sakoda S, Sawada T. Magnetic resonance spectroscopic study of Alzheimer's disease and frontotemporal dementia/Pick complex. Neuroreport. 2006;17(4):413–6.
24. Gogtay N. Principles of sample size calculation.Indian J Ophthalmol. 2010;58(6):517.

25. Agnollitto MISS, Leoni RF, Foss MP, Palaretti J, Cayres M, Pansarim V, et al. Influence of cerebral blood flow on volumetric loss related to Alzheimer's disease. Dement Neuropsychol. 2023;17:e20230004.
26. Jack CR Jr, Bennett DA, Blennow K, Carrillo MC, Dunn B, Haeberlein SB, et al. NIA-AA Research Framework: Toward a biological definition of Alzheimer's disease. Alzheimers Dement. 2018;14(4):535–562
27. Thropp P, Phillips E, Jung Y, Thomas DL, Tosun D, Alzheimer's Disease Neuroimaging Initiative. Arterial spin labeling perfusion MRI in the Alzheimer's Disease Neuroimaging Initiative: Past, present, and future. Alzheimer's & Dementia. 2024;20(12):8937–52.
28. Marterstock DC, Knott MF, Hoelter P, Lang S, Oberstein T, Kornhuber J, Doerfler A, Schmidt MA. Pulsed arterial spin labeling and segmented brain volumetry in the diagnostic evaluation of frontotemporal dementia, Alzheimer’s disease and mild cognitive impairment. Tomography. 2022;8(1):229–44.

Tables

Table 1. Baseline demographics and clinical characteristics of study participant

Variable	AD (n=15)	FTD (n=15)	Controls (n=15)	p-value
Age (years)	67.2 ± 6.1	62.5 ± 5.8	55.9 ± 7.3	<0.001
Male, n (%)	10 (66.7)	9 (60.0)	9 (60.0)	0.45
MMSE	20.4 ± 2.5	21.0 ± 2.2	28.7 ± 1.1	<0.001
MoCA	19.6 ± 2.8	20.2 ± 2.6	27.9 ± 1.3	<0.001

Table 2: Comparison of mean CBF values (ml/100g/min) on ASL between all groups

Region	Mean CBF in AD group (n=15)	Mean CBF in FTD group (n=15)	Mean CBF in Controls (n=15)	ANCOVA F-value (Group effect)	p-value (Group)	Age (Covariate) p-value
Right frontal	27.81±9.90	23.76±9.56	40.23±5.91	15.14	**<0.001**	0.26
Left frontal	29.67±10.74	25.64±10.20	40.62±6.23	12.08	**<0.001**	0.12
Right temporal	25.61±9.41	22.94±7.85	36.26±5.25	14.18	**<0.001**	0.12
Left temporal	26.75±10.73	23.14±7.59	36.15±5.54	11.26	**<0.001**	0.15
Right parietal	28.45±12.40	33.23±10.18	39.72±5.37	7.91	**0.001**	**0.03**
Left parietal	27.70±11.80	34.52±9.51	39.01±5.27	7.54	**0.002**	0.08
Right occipital	27.46±7.25	32.79±8.54	39.77±8.43	10.59	**<0.001**	0.09
Left occipital	27.78±7.95	33.61±8.84	39.79±9.10	10.23	**<0.001**	**0.03**
Right hippocampus	23.86±8.65	23.44±8.91	34.08±7.99	8.74	**<0.001**	0.15
Left hippocampus	24.02±9.47	26.05±7.79	33.23±4.97	6.68	**0.003**	0.24
Anterior cingulate	27.73±8.58	25.07±7.54	38.21±7.68	10.61	**<0.001**	0.62
Posterior cingulate	31.54±10.53	35.22±8.54	41.91±8.51	7.64	**0.002**	**0.03**

TABLE 3: Comparison of spectroscopic concentrations of the metabolites and their ratios (A=Anterior Cingulate Gyrus, P= Posterior Cingulate Gyrus, NS=Not significant)

Metabolites	AD (n=15)	FTD (n=15)	Controls (n=15)	ANCOVA F-value (Group effect)	p value (Group)	Age (Covariate) p-value
mI (A)	0.28±0.16	1.55±1.26	0.82±0.74	9.79	< 0.001	0.1
mI(P)	1.21±0.59	0.97±0.71	1.01±0.62	0.82	NS	0.46
NAA(A)	17.17±3.93	12.29±3.65	25.18±5.16	30.81	< 0.001	0.86
NAA(P)	14.54±6.69	17.26±5.44	24.78±3.46	13.38	< 0.001	0.46
Cr(A)	10.39±2.97	8.12±3.33	14.26±2.78	13.06	< 0.001	0.53
Cr(P)	9.89±3.51	11.64±3.45	14.31±2.15	5.5	0.008	0.7
NAA/mI(A)	38.17±25.11	7.78±6.94	33.20±29.85	8.27	0.001	0.12
NAA/mI(P)	10.85±10.30	10.98±5.97	23.55±17.66	3.43	0.04	0.38
mI/Cr(A)	0.06±0.07	0.46±0.62	0.10±0.13	5.69	0.007	0.14
mI/Cr(P)	0.28±0.31	0.18±0.14	0.11±0.07	3.43	0.04	0.38
NAA/Cr(A)	1.71±0.35	1.82±0.97	1.77±0.22	0.32	NS	0.28
NAA/Cr(P)	1.66±0.74	1.46±0.27	1.75±0.18	2.45	NS	0.06

Figures

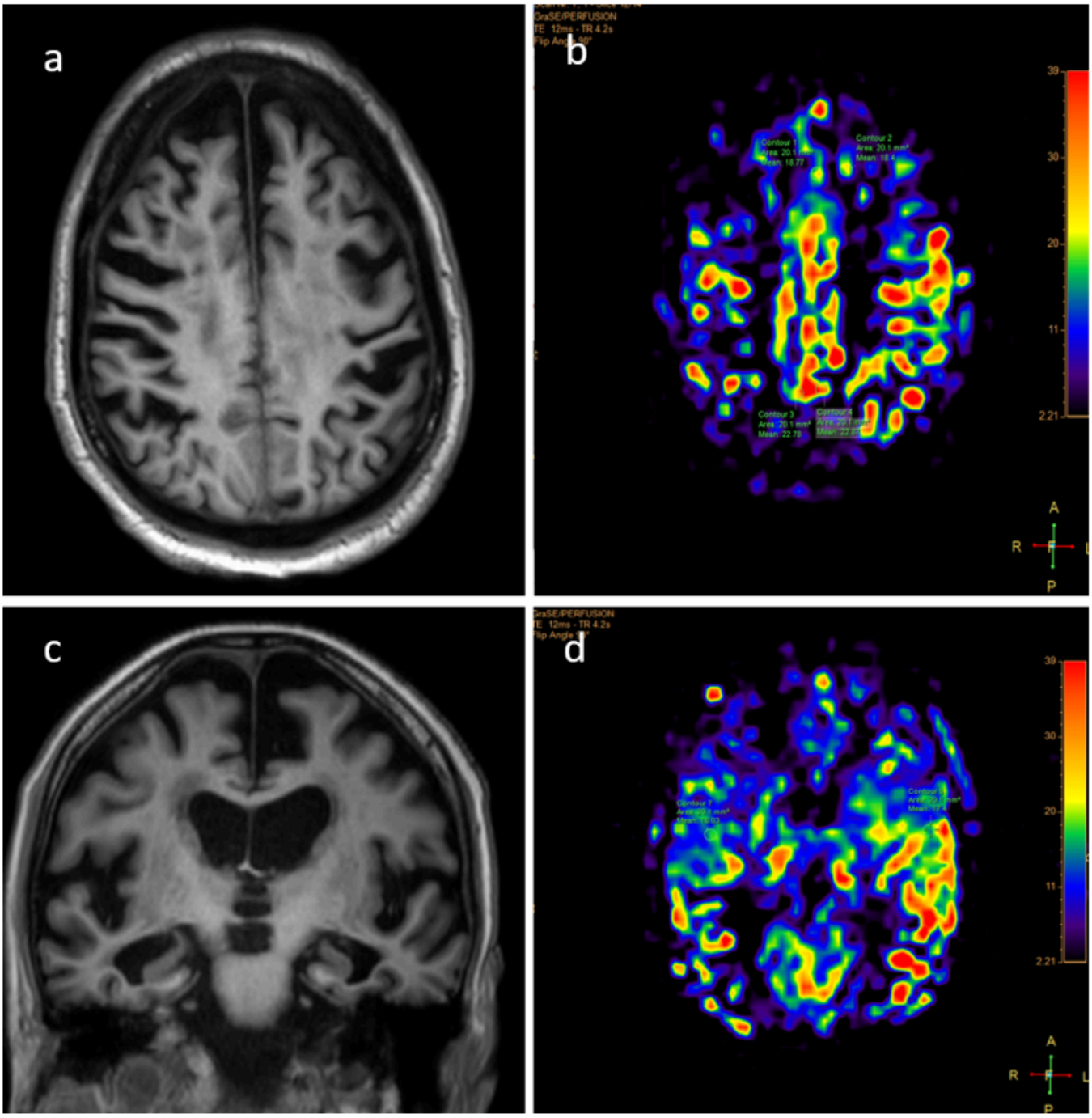


Figure 1

a) Axial T1 image showing bifrontal atrophy with thinning of gyri and enlarged sulcal spaces, b) corresponding frontal hypoperfusion on axial ASL-MRI image c) Coronal T1 image showing bilateral temporal atrophy with significantly expanded choroid fissure with temporal horn expansion and marked loss of hippocampal height d) Hypoperfusion in bilateral temporal lobes on axial ASL-MRI in FTD.

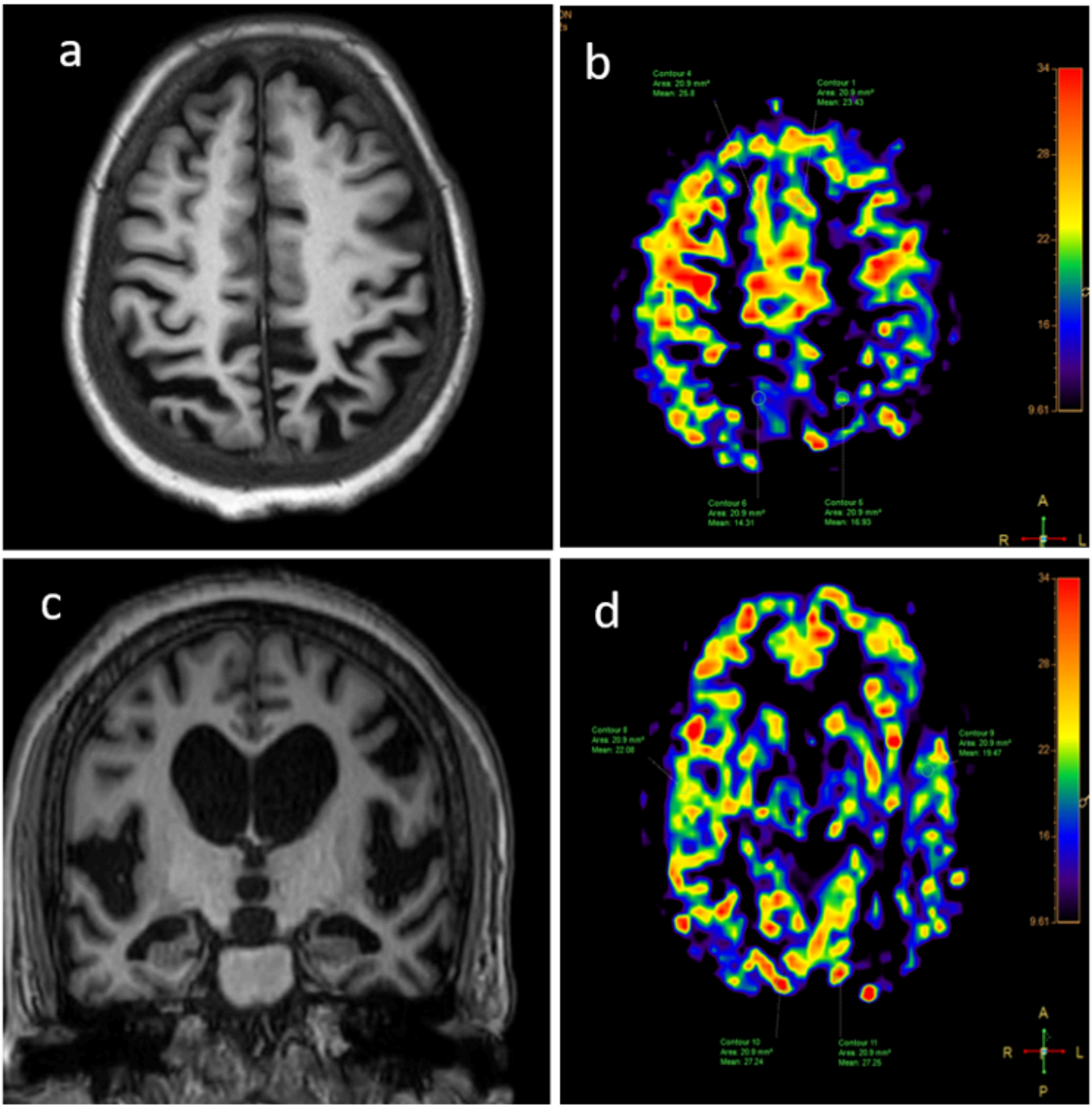


Figure 2

a) T1 axial images showing significant atrophy of the parietal lobes and pre-cuneus b) corresponding parietal hypoperfusion on axial ASL-MRI image c) Coronal T1 images showing bilateral temporal atrophy with expanded choroid fissure with temporal horn expansion and loss of hippocampal height d) Hypoperfusion in bilateral temporal lobes on axial ASL-MRI in AD.

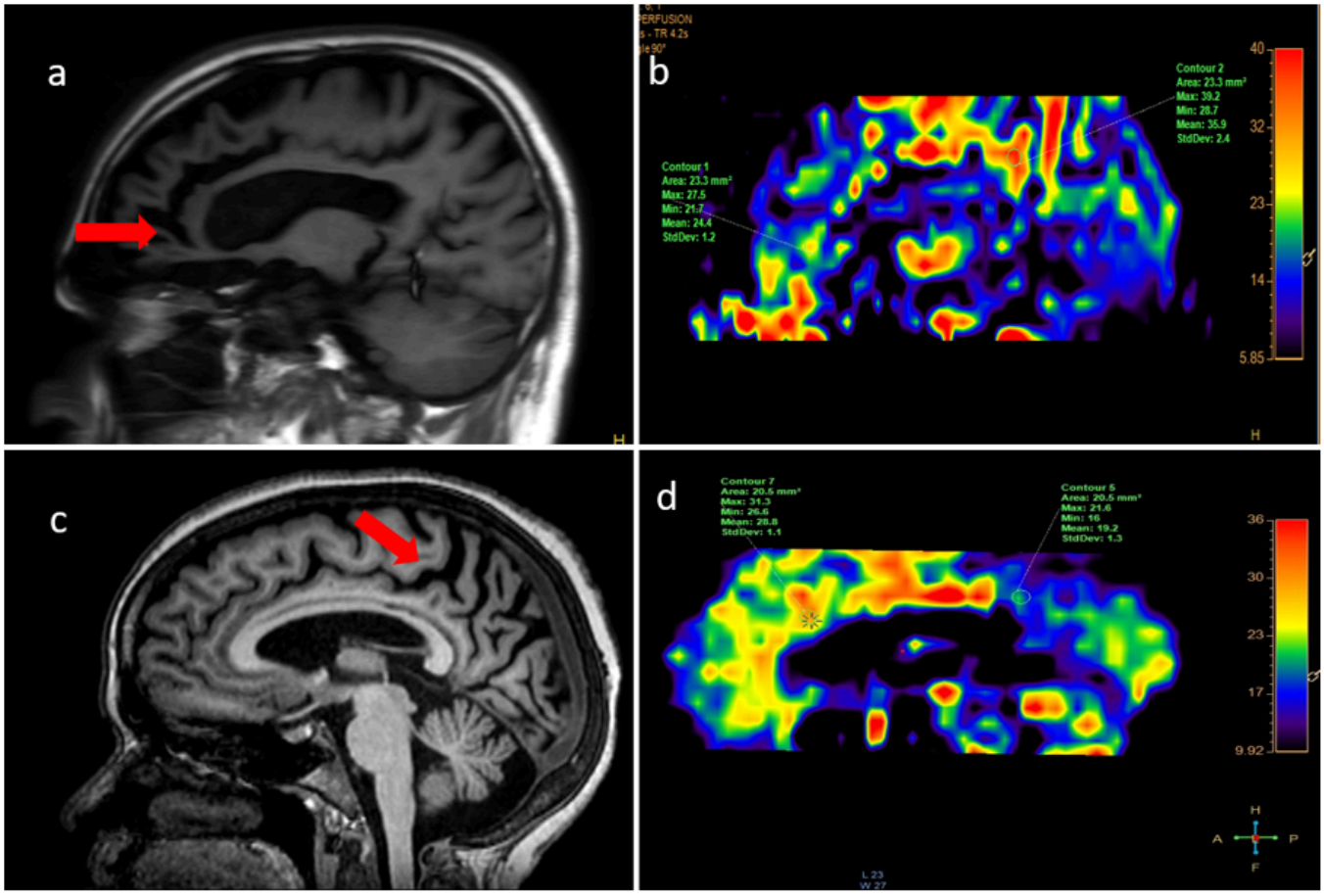


Figure 3

a) Sagittal T1 image showing widening of anterior cingulate sulcus and loss of volume in anterior cingulate gyrus with b) corresponding hypoperfusion in anterior cingulate gyrus compared to posterior cingulate gyrus on sagittal ASL-MRI images.

c) Sagittal T1 image showing widening and loss of volume of posterior cingulate sulcus with d) corresponding hypoperfusion in posterior cingulate gyrus compared to anterior cingulate gyrus on sagittal ASL-MRI images

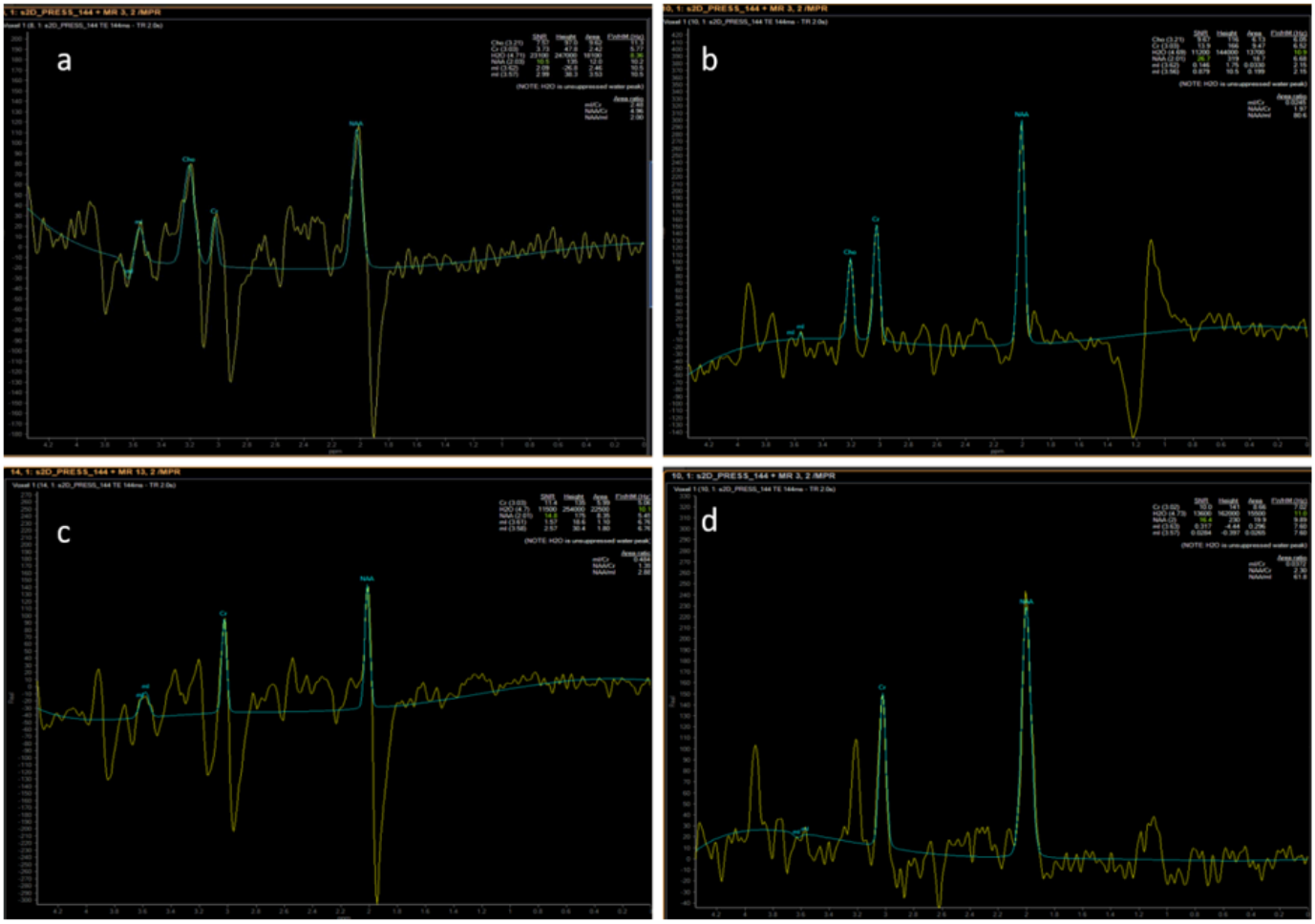


Figure 4

(a, b): MRS (multivoxel) images with voxel placement at anterior cingulate gyrus (a) showing increased concentration of mI, reduced NAA, reduced Cr, increased mI/Cr ratio, reduced NAA/Cr and reduced NAA/mI ratio in FTD compared to (b) healthy control with normal concentration of metabolites and ratios.

(c,d): MRS images with voxel placement at posterior cingulate gyrus: showing increased concentration of mI, reduced NAA, reduced Cr, increased mI/Cr ratio, reduced NAA/Cr and NAA/ mI ratio in AD compared to (b) healthy control with normal concentration of metabolites and ratios.

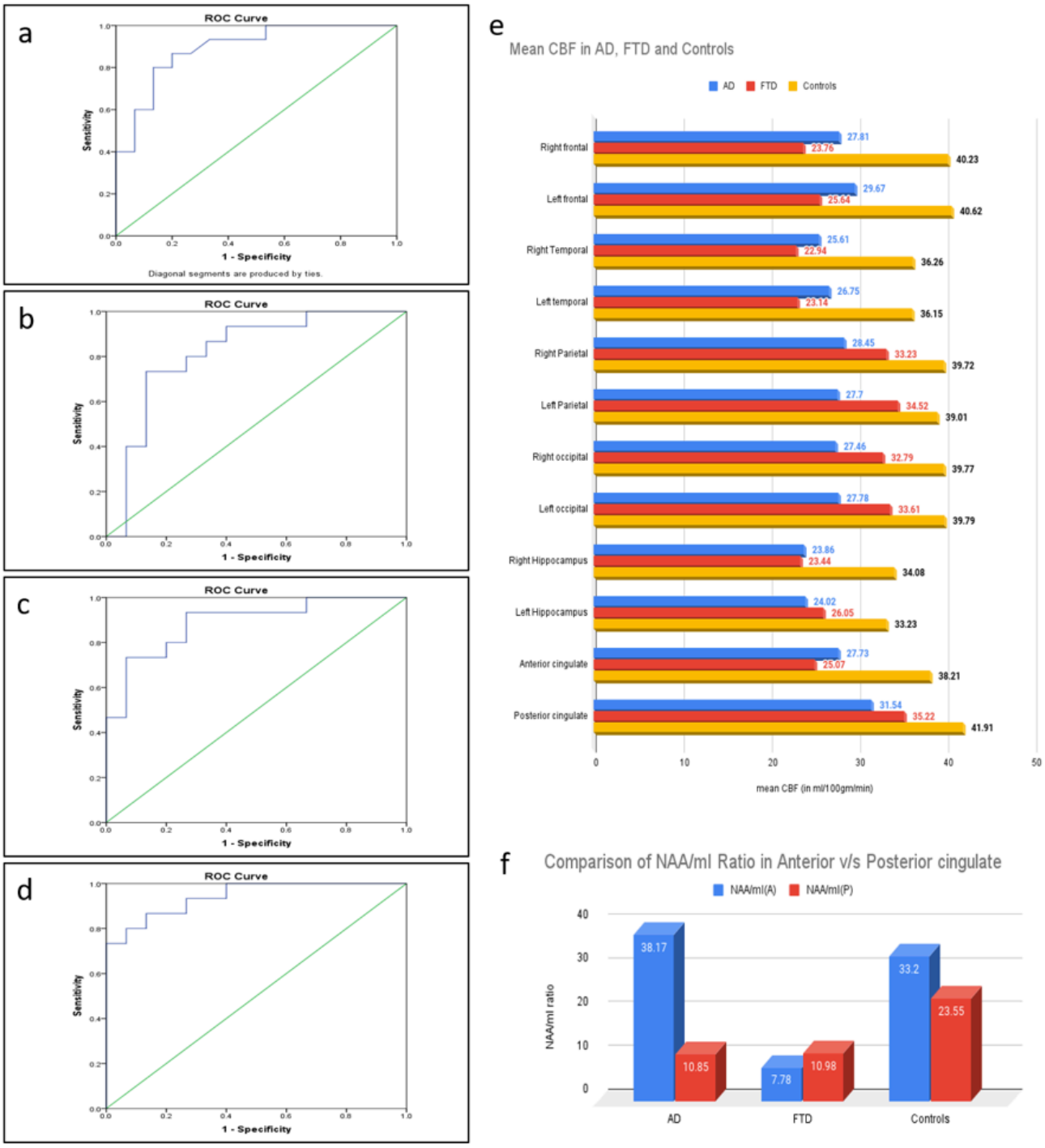


Figure 5

(a): ROC Curve using mean CBF in anterior cingulate gyrus CG (A) to differentiate between FTD and controls.

(b): ROC Curve using mean CBF in posterior cingulate gyrus CG (P) to differentiate between AD and controls

(c): ROC Curve using NAA/ml ratio in Anterior Cingulate gyrus to differentiate between FTD and healthy controls.

(d) ROC Curve using NAA/ml ratio in anterior Cingulate gyrus to differentiate between AD and FTD.

(e) Bar chart showing mean CBF in all four lobes, bilateral hippocampi, anterior cingulate gyrus and posterior cingulate gyrus in AD, FTD and controls.

(f): Column chart showing NAA/mI Ratio in anterior and posterior cingulate gyrus in all groups.